Supramolecular Differentiation for Construction of Anisotropic Fullerene Nanostructures by Time-Programmed Control of Interfacial Growth

Partha Bairi,[†,‡] Kosuke Minami,*[,†,‡] Jonathan P. Hill,[†] Waka Nakanishi,[†] Lok Kumar Shrestha,*[,†] Chao Liu,[§] Koji Harano,[§] Eiichi Nakamura,[§] and Katsuhiko Ariga*[,†]

[†] World Premier International Center for Materials Nanoarchitectonics (WPI-MANA), National Institute for Material Science (NIMS), 1-1 Namiki, Tsukuba, Ibaraki, 305-0044, Japan

[§] Department of Chemistry, The University of Tokyo, 7-3-1 Hongo, Bunkyo-ku, Tokyo, 113-0033, Japan

[‡] *These authors contributed equally to this work.*

* Correspondence and requests for materials should be addressed to K.M. (email: MINAMI.Kosuke@nims.go.jp), L.K.S. (email: SHRESTHA.Lokkumar@nims.go.jp) and K.A. (email: ARIGA.Katsuhiko@nims.go.jp).

Abstract

Supramolecular assembly can be used to construct a wide variety of ordered structures by exploiting the cumulative effects of multiple non-covalent interactions. However, the construction of anisotropic nanostructures remains subject to some limitations. Here we demonstrate the preparation of anisotropic fullerene-based nanostructures by supramolecular differentiation, which is the programmed control of multiple assembly strategies. We have carefully combined interfacial assembly and local phase separation phenomena. Two fullerene derivatives, **PhH** and **C12H** were together formed into self-assembled anisotropic nanostructures by using this approach. This technique is applicable for the construction of anisotropic nanostructures without requiring complex molecular design or complicated methodology.

Keywords: carbon nanostructures; fullerenes; self-assembly; nanostructure; liquid–liquid interface

Many of the constituents of natural systems including molecules, biomolecules and cells are composed of asymmetric structures. This asymmetry is an extremely important feature and it is maintained even through complex processes such as embryonic cleavage where asymmetric cell division events lead to embryo development from a zygote under control by cellular differentiation.[1] However, processes of self-assembly in chemistry often only yield simple symmetric nanostructures, such as lamellae, dimensionless particles or spheres, due to energy minimization processes. The construction of asymmetric nanostructures requires additional information which can be incorporated by applying molecular design principles, such as can be found in finely tuned complex molecules or polymers where phase separation processes can be affected by designing non-covalent interactions including electrostatic, hydrophilic–hydrophobic, hydrogen bonding, dipole–dipole or π-π interactions.[2–8]

Liquid–liquid interfacial assembly has great potential for the synthesis of asymmetric forms.[9] By using this technique, different aspects of anisotropic nanostructures, including particle dimensions and morphology, can be controlled by applying different external stimuli, such as solvent combinations, temperature and incubation time. However, there remain some limitations of these approaches in the fabrication of anisotropic nanostructures. Through a combination of the phase separation and interfacial assembly techniques, anisotropic structures containing specifically designed components can be constructed. We have coined the term "supramolecular differentiation" (Figure 1) for this process.

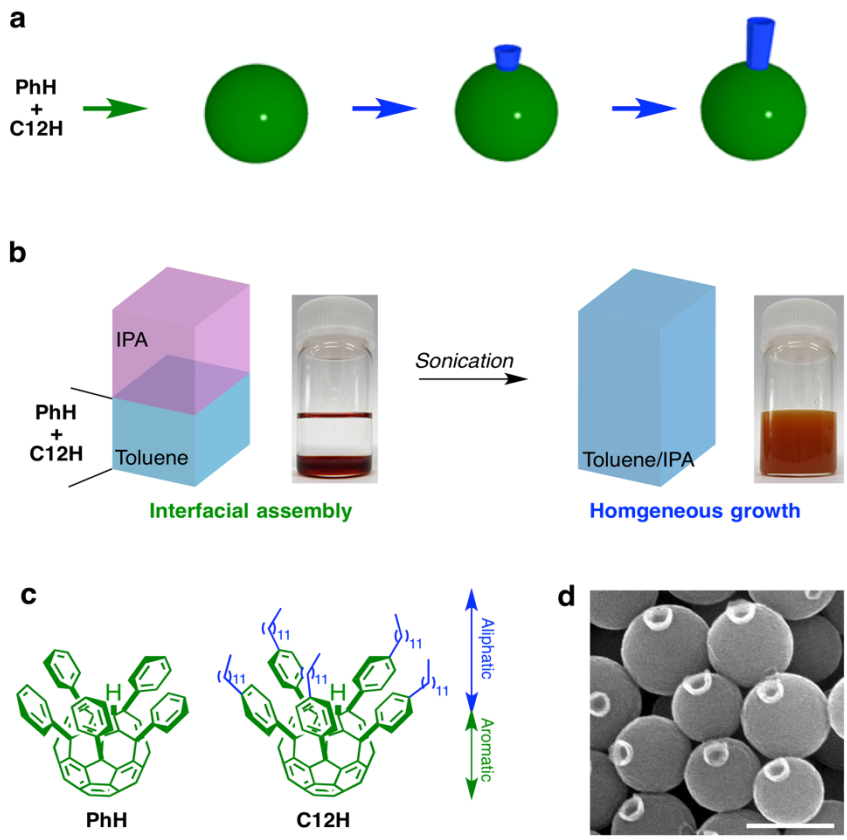

Figure 1. Supramolecular differentiation for preparation of self-assembled anisotropic fullerene nanostructures. Schematic illustrations of (a) supramolecular differentiation and (b) ULLIP method. (c) Structures of **PhH** and **C12H**. (d) SEM image of anisotropic fullerene nanostructures. Scale bar is 1 μm.

Fullerene is a zero-dimensional molecule which possesses interesting properties including high hydrophobicity due to strong van der Waals and π-π interactions derived from its fused π-conjugated structure.[10–14] Even simple fullerene derivatives with seemingly insignificant functionalities have been shown to form a wide variety of self-assembled structures, such as particles,[15–23] fibers,[20,24,25] micelles,[26–28] vesicles[29–35] and liquid crystals.[36–40] We speculated that liquid–liquid interfacial assembly and homogeneous growth could be finely programmed for supramolecular differentiation under control by the local phase separation between aromatic fullerene core and aliphatic substituents of fullerene derivatives, and hence used for the construction of asymmetric nanostructures. Here we demonstrate the synthesis of an anisotropic fullerene nanostructure by combining the liquid–liquid interfacial assembly method with local phase separation of two fullerene derivatives:

pentakis(phenyl)fullerene (**PhH**),[22,41] and pentakis(4-dodecylphenyl) fullerene (**C12H**)[30] (Figure 1c). Of these two compounds, it is notable that the aliphatic substituents of **C12H** are capable of inducing local phase separation at a liquid–liquid interface.[38]

Results and Discussion

Preparation of anisotropic fullerene nanostructures. Supramolecular nanoarchitectures of fullerene derivatives were prepared by an ultrasonic liquid–liquid interfacial precipitation (ULLIP) method, which is the standard procedure for the preparation of pristine fullerene nanocrystals. A poor solvent for fullerenes (*e.g.*, isopropanol) is added slowly to a solution of fullerenes (in a good solvent such as toluene), and then sonication is applied (Figure 1b).[42–46] Fullerene derivatives, **PhH** and **C12H**, were synthesized and purified using previously reported methods.[30,41] Both fullerene penta-adducts are highly soluble in aromatic solvents, such as toluene, but are insoluble in polar solvents, such as alcohols. Poor solvent isopropanol was slowly added to a solution of fullerene penta-adducts in toluene to form a liquid–liquid interface. After a brief pre-incubation time (t_{before}) of 1 h, sonication was applied to the mixture leading to a homogeneous solution of toluene and isopropanol, then the resulting solution was further incubated for an additional 48 h (incubation time, t_{after}). ULLIP using **PhH** only contains spherical structures with diameters 199 ± 44 nm determined by scanning electron microscopy (SEM) measurements, whereas **C12H** did not show any nanostructures (Figures 2a and S1). Mixing **PhH** and **C12H** ([**PhH**]:[**C12H**] = 2:1) and applying the ULLIP resulted in spontaneous formation of anisotropic structures of spherical particles bearing tube-like protuberances on their surfaces (Figure 2b). Powder XRD patterns of the **PhH**:**C12H** nanostructures contained only a broad peak, indicating that they were in a non-crystalline amorphous state (Figure 2d). Spherical particle structures were not observed if a dropcasting method, where the toluene solution of the mixture of **PhH** and **C12H** was dropped onto the substrate then dried at 80 °C (Figure S2), was used. This indicates that formation of the spherical core structures requires the liquid–liquid interfacial assembly process. The size of the core particles can be fine-tuned by changing the ratio of **PhH** and **C12H**. Increasing the content of **C12H** from 0 to 60% leads to a linearly proportional increase in the size of the particles from 199 ± 44 nm to 1.32 ± 0.27 μm (Figures 2c,e and S4, histogram of the core particle size). Remarkably, all the **PhH**:**C12H** nanostructures have a single tube-like protuberance on

their surfaces. Between the ratio of **C12H** vs. **PhH** ([**C12H**]/[**PhH**]) at 0.5 and 0.75, a single tube-like structure was observed on the surfaces of the particles. At ratios less than 0.5, the tube-like structures were not observed. In contrast, multiple tube-like structures were formed on the surfaces of particles at ratios greater than 1.0 (Figure S5). From these observations, we surmise that the number of tube-like structures is dependent on the concentration of **C12H**.

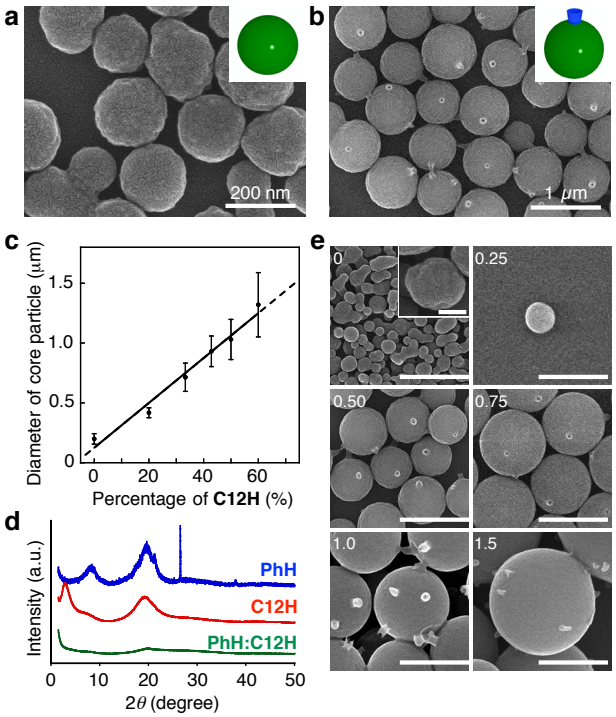

Figure 2. Fullerene nanoarchitectures of **PhH** and **C12H**. SEM images of nanostructures of (a) **PhH** and (b) **PhH**:**C12H** prepared by ULLIP ([**C12H**]/[**PhH**] = 0.5). c) Ratio of **C12H** vs **PhH** affecting the diameter of the core particles. d) Powder XRD measurements of **PhH** (blue), **C12H** (red) and **PhH**:**C12H** aggregates (green). e) SEM images of the **PhH**:**C12H** nanostructures of different ratio of **PhH** and **C12H** from 0 to 1.5. Scale bars are 1 μm. Inset shows a magnification (scale bar in inset: 100 nm).

Control of interfacial assembly and homogeneous growth over time before and after sonication. The construction of anisotropic structures requires precise control of the liquid–liquid interfacial assembly process and the homogeneous growth, which can be achieved by varying incubation time prior to sonication (t_{before}). When t_{before} is less than 1 h, the formation of core particles was not complete and the particles were

fused, possibly due to the premature loss of the confining medium of the liquid–liquid interface before nucleation of stable seed particles had occurred (Figure 3a,c). Despite the incomplete formation of the core, some of the aggregated **PhH**:**C12H** nanostructures still contained the single tube-like structures on their surfaces (Figure 3b, white arrows). In contrast, when t_{before} was more than 3 h, formation of the core particles was complete but particles obtained possessed multiple tube-like structures (Figure 3b). For longer durations of t_{before} and without applying sonication in the liquid–liquid interfacial precipitation (*i.e.*, LLIP) method,[42] formation of **PhH**:**C12H** nanostructures with multiple tube-like structures was observed (Figure 3b). The sizes of core particles for t_{before} = 3 h and for the LLIP method increased from 714 ± 118 to 874 ± 199 and 1397 ± 159 nm, respectively. This is similar to what was observed for the formation of **PhH**:**C12H** particles at higher compound ratios ([**C12H**]/[**PhH**] ≥ 1.0) (see Figure 2c). These results suggest that the number of tube-like structures is related to the diameters of the core particles which is in turn controlled by setting the pre-incubation time t_{before} prior to sonication.

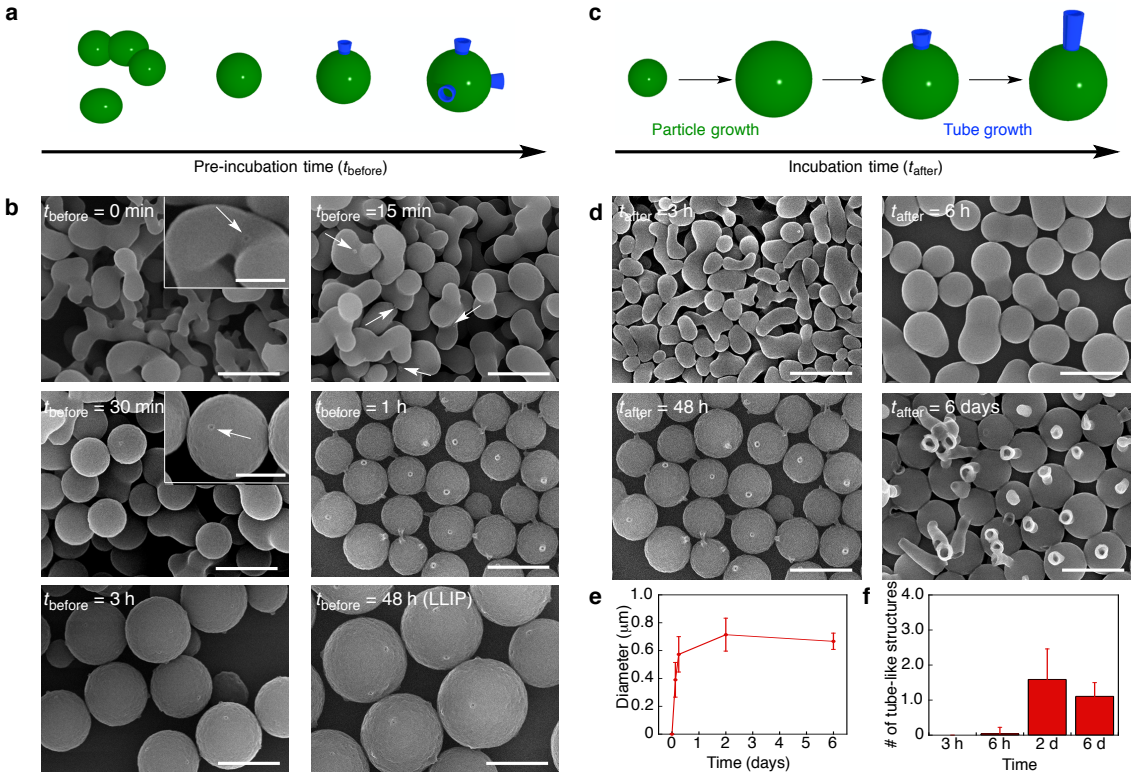

Figure 3. Self-assembled anisotropic **PhH**:**C12H** nanostructures. a,c) Pre-incubation time (t_{before})-dependent (a) and the incubation time (t_{after})-dependent (c) formations of anisotropic fullerene nanostructure. b) SEM images of pre-incubation time-dependent

formation nanostructures. t_{before} = 0 min, 15 min, 30 min, 1 h and 3 h of ULLIP, and LLIP methods. Scale bars are 1 μm. Scale bars in inset images are 400 nm. d) SEM images of incubation time-dependent formation of **PhH**:**C12H** nanostructures. t_{after} = 3 h, 6 h, 48 h and 6 days. Scale bars are 1 μm. e,f) Incubation time-dependent changes of diameter of the core particles (e) and the number of tube-like structures on the surface (f). Error bars indicate ±standard deviation.

We subsequently investigated the processes involved in the formation of the tube-like structures. Isopropanol was slowly added to a mixture of **PhH** and **C12H** ([**PhH**]:[**C12H**] = 2:1) in toluene to form a liquid–liquid interface with the pre-incubation time t_{before} fixed at 1 h. For different incubation times after sonication (t_{after}), the diameters of core particles and numbers of tube-like structures per particle were analyzed by SEM measurements. For all values of t_{after}, formation of particles was observed (Figure 3d). Diameters of the particles initially increased reaching a plateau at ca. 700 nm from t_{after} ~ 48 h (Figure 3e). The tube-like structures were not observed at t_{after} = 6 h (Figure 3d,e). When t_{after} was increased to 6 days, the tube-like structures were significantly elongated on the surface (Figure 3d). These results indicate an initial formation of the core particles followed by growth of the tube-like structures on their surfaces. Notably, the number of tube-like structures at t_{after} = 6 days is unchanged (Figure 3f) and, in particular, does not increase. This feature strongly suggests that the formation of the tube-like structures is programmed at an initial stage during pre-incubation t_{before} and the tube-like structures can form only at certain positions on the particles' surfaces.

Mechanism of formation of anisotropic fullerene nanostructures. As the diameters of the core particles increased both when **C12H** content was high (Figure 2; [**C12H**]/[**PhH**] > 1.0) and when pre-incubation time was long (Figure 3; t_{before} > 3 h), the number of tube-like structures also increased, whereas the number of tube-like structures was retained during the homogeneous growth occurring after sonication. Thus, it is thought that the domains necessary for formation of the tube-like structures are formed on the seed particles during the interfacial growth process, and also that formation of the domain structures cannot occur after sonication has been performed. Because of the lower solubility of **PhH** relative to **C12H**,[30] **PhH** initially forms seed

particles during interfacial growth. The surfaces of the seed particles can provide a substrate for formation of the domain structures required for formation of the tube-like structures. As the concentration of **C12H** increased (Figure 2), the diameters of the core particles also increased with a concurrent increase in the number of tube-like structures. It is likely that domains of alkylated fullerene **C12H** form on the seed particles because of the aromatic/aliphatic phase separation caused by solvophobic forces generated by the immiscibility of C_{60} and alkyl chains.[38,47]

Although a detailed mechanism for the formation of **PhH**:**C12H** particles bearing a tube-like structure remains unclear, based on the results presented here, we propose the following mechanism (Figure 4): formation of the tube-like structures is programmed during the liquid–liquid interfacial assembly procedure when seed particles are initially formed at the liquid–liquid interface. The tube-like structures cannot form if the concentration of **C12H** is too low (Figure 4a, particle I), possibly because local phase-separation cannot occur on the seed particles during the interfacial growth. This suggests that the domain structure necessary to act as scaffold for the formation of the tube-like structures cannot form on the seed particles (Figure 2). Following sonication, tube-like structures can also not form on the surface of the aggregated structures (Figure 4b, path A). If t_{before} is too short (Figure 3b; $t_{before} < 30$ min), the domain structures can also not form on the seed particles, possibly because the concentration of **C12H** is not high enough lead to a local phase-separation on the seed particle during the interfacial growth process. If t_{before} is increased (Figure 4a, particles II and III) then the local phase-separation on the seed particles can occur leading to formation of a single domain structure on the seed particles. When t_{before} is 1 h (Figure 3) or the ratio between **PhH** and **C12H** is 0.5 to 0.75 (Figure 2e; see also Figure S4), seed particles contain a sufficient quantity of **C12H** so that formation of a single domain on the seed particle can occur (Figure 4a, particle II). Thus, after sonication a single tube-like structure can form on the surface (Figure 4b, path B). However, when t_{before} is more than 3 h or the ratio of **PhH** and **C12H** is higher than 1.0, (Figure 4a, particle III), the amount of **C12H** on the seed particles is sufficient for formation of multiple domains on their surfaces, and consequently formation of multiple tube-like structures during the homogeneous growth stage (Figure 4b, path C) is observed. The detailed structures of the core particles and tube-like structures are unclear since they appear amorphous. Despite this, the precise control of the formation of seed particle by

changing interfacial growth and homogeneous growth can be tuned by supramolecular differentiation.

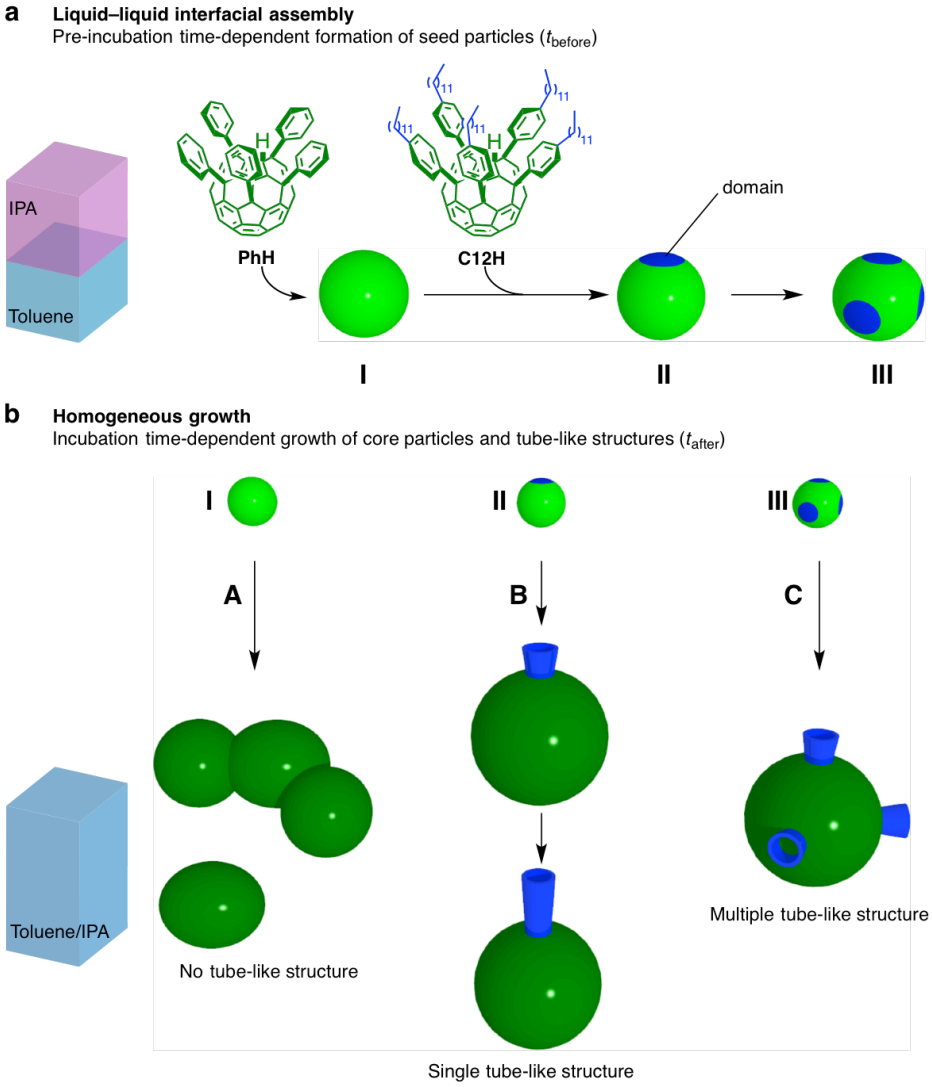

Figure 4. Schematic illustration of proposed mechanism of particle growth Liquid–liquid interfacial assembling process. a) Liquid–liquid interfacial assembly of a seed particle and domain structures for formation of tube-like structures before applying sonication. b) Homogeneous growth of particles and tube-like structures on the domain after applying sonication.

Conclusion

In conclusion, we have succeeded in constructing anisotropic fullerene nanoarchitectures by using supramolecular differentiation, which might be considered analogous with embryonic development but applied in the field of material science. We

have finely tuned the local phase separation by means of time-programmed control of the liquid–liquid interfacial assembly and homogeneous growth. In contrast, homogeneous growth alone leads to formation of spherical particles.[22] This fullerene anisotropic nanostructure will provide a great variety of opportunities in a wide range of applications in materials science, including in electronic devices, sensors and biomaterials.[48–50] Our technique, which is essentially a combination of the interfacial assembly and phase separation phenomena, can be used to further enable the construction of anisotropic nanostructures.

Experimental Section

Preparation of PhH:C12H nanostructures. PhH and **C12H** were synthesized and purified by using previously reported methods.[30,41] Briefly, the respective Grignard reagent (6.00 mmol) in THF (ca. 1.0 M) was added to a suspension of $CuBr{\cdot}SMe_2$ (1.23 g, 6.00 mmol) in THF (3 mL) at 35 °C. After stirring for 10 min at 35 °C, a solution of C_{60} (361mg, 0.502 mmol) in 1,2-dichlorobenzene (16.2 mL) was added to the suspension. After stirring for 1 h at 35 °C, a saturated aqueous solution of ammonium chloride (1 mL) was added to the suspension. The suspension was stirred under reduced pressure to remove THF and dimethyl sulfide. The concentrated mixture was filtered/washed through pads of silica gel and celite with CS_2. The filtrate was concentrated under reduced pressure until precipitation occurred. Methanol was then added until precipitation was complete. The precipitate was collected by filtration, washed with methanol, and dried under reduced pressure overnight to obtain an orange powder.

Fullerene anisotropic nanostructures were prepared by the liquid–liquid interfacial precipitation (LLIP) method.[42] Stock solutions were prepared by separately dissolving **PhH** (30 mg) and **C12H** (30 mg) in 10 mL each of toluene with ultrasonication for about 30 min. In a typical procedure, the mixture of **PhH** and **C12H** at selected molar ratio was taken in a thoroughly cleaned 13.5 mL glass vial and incubated at 15 °C. A liquid–liquid interface was prepared by slowly adding isopropyl alcohol (IPA, 5 mL), which had been incubated at 15 °C for more than 1 h, onto the toluene solution of fullerenes. The mixture was then incubated at 15 °C for 48h. For the ultrasonic liquid–liquid interfacial precipitation (ULLIP) method,[43,44,47] after preparing an interface, the mixture was stored at 15 °C for 1 h (pre-incubation time, t_{before}) without

disturbance. After 1 h, sonication was applied for 30 s followed by a light shaking by hand. The resulting mixture was again stored at 15 °C in an incubator for an additional 48 h.

Scanning electron microscopy. Scanning electron microscopy (SEM) images of the fullerene anisotropic nanostructures were obtained using a Hitachi Model S-4800 field effect scanning electron microscope (FE-SEM) operating at an accelerating voltage of 10 kV. All the samples for SEM were prepared by dropping a suspension of fullerene anisotropic nanostructures onto passivated silicon substrates followed by drying at 80 °C. The samples were coated with platinum (ca. 2 nm) by sputtering using a Hitachi S-2030 ion coater.

Powder X-ray diffraction. Powder X-ray diffraction (XRD) patterns were recorded at room temperature (25 ºC) on a Rigaku RINT2000 diffractometer using Cu-Kα radiation (λ = 0.1541 nm). For recording the XRD pattern, toluene solution of **C12H** and freshly prepared anisotropic nanostructure were drop casted on a glass substrate and dried at 80 ºC. In case of **PhH**, solid powder was placed on a glass substrate and XRD pattern was recorded at 25 ºC.

Acknowledgement

This work was partly supported by World Premier International Research Center Initiative (WPI Initiative), MEXT, Japan, and Japan Society for the Promotion of Science (JSPS) KAKENHI Grant Number 26104541, 15H05754 and 15K17890. K.M. thank YAMATO-MANA program from NIMS.

Author contributions

K.M. and L.K.S. conceived and designed research. P.B., K.M. and L.K.S. performed the experiments. P.B., K.M. and L.K.S. analyzed data. K.M., L.K.S., J.P.H. and K.A. wrote the manuscript. All authors discussed the results and commented on the manuscript.

Additional Information

Supporting Information Available; The Supporting Information is available free of charge on the ACS Publications website at DOI: 10.1021/XXX.

Additional SEM images and statistical analysis data (PDF)

Competing financial interests: The authors declare no competing financial interests.

Reference

1. Alberts, V. B.; Johnson, A.; Lewis, J.; Raff, M.; Roberts, K.; Walter, P. *Molecular Biology of the Cell*, 3rd Ed., Garland Publishing Inc. 1994.
2. Mukhopadhyay, R. D.; Ajayaghosh, A. Living Supramolecular Polymerization. *Science* **2015**, *349*, 241–242.
3. Mukhopadhyay, R. D.; Praveen, V. K.; Hazra, A.; Maji, T. K.; Ajayaghosh, A. Light Driven Mesoscale Assembly of a Coordination Polymeric Gelator into Flowers and Stars with Distinct Properties. *Chem. Sci.* **2015**, *6*, 6583–6591.
4. Noorduin, W. L.; Grinthal, A.; Mahadevan, L; Aizenberg, J. Rationally Designed Complex, Hierarchical Microarchitectures. *Science* **2013**, *340*, 832–837.
5. Aida, T.; Meijer, E. W.; Stupp, S. I. Functional Supramolecular Polymers. *Science* **2012**, *335*, 813–817.
6. Miyako, E.; Kono, K.; Yuba, E.; Hosokawa, C.; Nagai, H.; Hagihara, Y. Carbon Nanotube-Liposome Supramolecular Nanotrains for Intelligent Molecular-Transport Systems. *Nat Commun.* **2012**, *3*, 1226.
7. Wang, C.; Wang, Z.; Zhang, X. Amphiphilic Building Blocks for Self-Assembly: From Amphiphiles to Supra-Amphiphiles. *Acc. Chem. Res.* **2012**, *45*, 608–618.
8. Van Esch, J. H. Supramolecular Chemistry: More than the Sum of its Parts. *Nature* **2010**, *466*, 193–194.
9. Li, W.; Yue, Q.; Deng, Y.; Zhao, D. Ordered Mesoporous Materials Based on Interfacial Assembly and Engineering. *Adv. Mater.* **2013**, *25*, 5129–5152.

10. Guillon, D.; Donnio, B.; Deschenaux R. In *Supramolecular Chemistry of Fullerenes and Carbon Nanotubes;* Martín, N., Nierengarten, J.-F., Eds. Wiley-VCH, 2012, pp 203–235.
11. Shrestha, L. K.; Ji, Q.; Mori, T.; Miyazawa, K.; Yamauchi, Y.; Hill, J. P.; Ariga, K. Fullerene Nanoarchitectonics: From Zero to Higher Dimensions. *Chem.–Asian J.* **2013**, *8*, 1662–1679.
12. Nakanishi, T. Supramolecular Soft and Hard Materials Based on Self-Assembly Algorithms of Alkyl-Conjugated Fullerenes. *Chem. Commun.* **2010**, *46*, 3425–3426.
13. Asanuma, H.; Li, H.; Nakanishi, T.; Möhwald, H. Fullerene Derivatives That Bear Aliphatic Chains as Unusual Surfactants: Hierarchical Self-Organization, Diverse Morphologies, and Functions. *Chem.–Eur. J.* **2010**, *16*, 9330–9338.
14 Nakamura, E.; Isobe, H. Functionalized Fullerenes in Water. The First 10 Years of Their Chemistry, Biology, and Nanoscience. *Acc. Chem. Res.* **2003**, *36*, 807–815.
15. Nakanishi, T.; Schmitt, W.; Michinobu, T.; Kurth, D. G.; Ariga, K. Hierarchical Supramolecular Fullerene Architectures with Controlled Dimensionality. *Chem. Commun.* **2005**, 5982–5984.
16. Isobe, H.; Nakanishi, W.; Tomita, N.; Jinno, S.; Okayama, H.; Nakamura, E. Gene Delivery by Aminofullerenes: Structural Requirements for Efficient Transfection. *Chem.–Asian J.* **2006**, *1–2*, 167–175.
17. Nakanishi, T.; Ariga, K.; Michinobu, T.; Yoshida, K.; Takahashi, H.; Teranishi, T.; Möhwald, H. G.; Kurth, D. Flower-Shaped Supramolecular Assemblies: Hierarchical Organization of a Fullerene Bearing Long Aliphatic Chains. *Small* **2007**, *3*, 2019–2023.

18. Maeda-Mamiya, R.; Noiri, E.; Isobe, H.; Nakanishi, W.; Okamoto, K.; Doi, K.; Sugaya, T.; Izumi, T.; Homma, T.; Nakamura, E. *In Vivo* Gene Delivery by Cationic Tetraamino Fullerene. *Proc. Natl. Acad. Sci. U.S.A.* **2010**, *107*, 5339–5344.

19. Zhang, X.; Nakanishi, T.; Ogawa, T.; Saeki, A.; Seki, S.; Shen, Y.; Yamauchi, Y.; Takeuchi, M. Flowerlike Supramolecular Architectures Assembled from C_{60} Equipped with a Pyridine Substituent. *Chem. Commun.* **2010**, *46*, 8752–8754.

20. Hizume, Y.; Tashiro, K.; Charvet, R.; Yamamoto, Y.; Saeki, A.; Seki, S.; Aida T. Chiroselective Assembly of a Chiral Porphyrin-Fullerene Dyad: Photoconductive Nanofiber with a Top-Class Ambipolar Charge-Carrier Mobility. *J. Am. Chem. Soc.* **2010**, *132*, 6628–6629.

21. Yang, X.; Zhang, G.; Zhang, D.; Xiang, J.; Yang G.; Zhua, D. Self-Assembly of a New C_{60} Compound with a *L*-Glutamid-Gerived Lipid Unit: Formation of Organogels and Hierarchically Structured Spherical Particles. *Soft Matter* **2011**, *7*, 3592–3598.

22. Nakamura, E.; Harano, K.; Inakoshi, N.; Liu, C. (The University of Tokyo, Towa Phamacetical Co., Ltd.) Water-Dispersible Amorphous Particles and Method for Preparing Same. WO 2015137289 A1, 2015.

23 Minami, K.; Okamoto, K.; Doi, K.; Harano, K.; Noiri, E.; Nakamura, E. siRNA Delivery Targeting to the Lung *via* Agglutination-Induced Accumulation and Clearance of Cationic Tetraamino Fullerene. *Sci. Rep.* **2014**, *4*, 4916.

24. Georgakilas, V.; Pellarini, F.; Prato, M.; Guldi, D. M.; Melle-Franco, M.; Zerbetto, F. Supramolecular Self-Assembled Fullerene Nanostructures. *Proc. Natl. Acad. Sci. U.S.A.* **2002**, *99*, 5075–5080.

25. Hollamby, M. J.; Karny, M.; Bomans, P. H. H.; Sommerdijk, N. A. J. M.; Saeki, A.;

Seki, S.; Minamikawa, H.; Grillo, I.; Pauw, B. R. Brown, P.; Eastoe, J.; Möhwald, H.; Nakanishi, T.; Directed Assembly of Optoelectronically Active Alkyl–π-Conjugated Molecules by Adding *n*-Alkanes or π-Conjugated Species. *Nat. Chem.* **2014**, *6*, 690–696.

26. Burghardt, S.; Hirsch, A.; Schade, B.; Ludwig, K.; Böttcher, C. Switchable Supramolecular Organization of Structurally Defined Micelles Based on an Amphiphilic Fullerene. *Angew. Chem. Int. Ed.* **2005**, *44*, 2976–2979.
27. Isobe, H.; Cho, K.; Solin, N.; Werz, D. B.; Seeberger, P. H.; Nakamura, E. Synthesis of Fullerene Glycoconjugates *via* a Copper-Catalyzed Huisgen Cycloaddition Reaction. *Org. Lett.* **2007**, *9*, 4611–4614.
28. Nitta, H.; Minami, K.; Harano, K.; Nakamura, E. DNA Binding of Pentaamino[60]fullerene Synthesized using Click Chemistry. *Chem. Lett.* **2015**, *44*, 378–380.
29. Homma, T.; Harano, K.; Isobe, H.; Nakamura, E. Nanometer-Sized Fluorous Fullerene Vesicles in Water and on Solid Surfaces. *Angew. Chem. Int. Ed.* **2010**, *49*, 1665–1668.
30. Homma, T.; Harano, K.; Isobe, H.; Nakamura, E. Preparation and Properties of Vesicles Made of Nonpolar/Polar/Nonpolar Fullerene Amphiphiles. *J. Am. Chem. Soc.* **2011**, *133*, 6364–6370.
31. Sawamura, M.; Nagahama, N.; Toganoh, M.; Hackler, U. E.; Isobe, H.; Nakamura, E.; Zhou, S.-Q. Chu B. Pentaorgano[60]fullerene $R_5C_{60}^-$. A Water Soluble Hydrocarbon Anion. *Chem. Lett.* **2000**, *29*, 1098–1099.
32. Zhou, S. Q.; Burger, C.; Chu, B.; Sawamura, M.; Nagahama, N.; Toganoh, M.; Hackler, U. E.; Isobe, H.; Nakamura, E. Spherical Bilayer Vesicles of Fullerene

Based Surfactants in Water: A Laser Light Scattering Study. *Science* **2001**, *291*, 1944–1947.

33. Isobe, H.; Homma T.; Nakamura, E. Energetics of Water Permeation through Fullerene Membrane. *Proc. Natl. Acad. Sci. U.S.A.* **2007**, *104*, 14895–14898.
34. Harano, K.; Minami, K.; Noiri, E.; Okamoto, K.; Nakamura, E. Protein-Coated Nanocapsules *via* Multilevel Surface Modification. Controlled Preparation and Microscopic Analysis at Nanometer Resolution *Chem. Commun.* **2013**, *49*, 3525–3527.
35. Harano, K.; Narita, A.; Nakamura, E. Photo-cross-linking of Exterior of Fullerene Bilayer that Prevents Vesicle Aggregation. *Chem. Lett.* **2014**, *43*, 877–879.
36. Sawamura, M.; Kawai, K.; Matsuo, Y.; Kanie, K.; Kato, T.; Nakamura, E. Stacking of Conical Molecules with a Fullerene Apex into Polar Columns in Crystals and Liquid Crystals. *Nature* **2002**, *419*, 702–705.
37. Matsuo, Y.; Muramatsu, A.; Kamikawa, Y.; Kato, T.; Nakamura, E. Synthesis and Structural, Electrochemical, and Stacking Properties of Conical Molecules Possessing Buckyferrocene on the Apex. *J. Am. Chem. Soc.* **2006**, *128*, 9586–9587.
38. Zhong, Y.-W.; Matsuo, Y.; Nakamura E. Lamellar Assembly of Conical Molecules Possessing a Fullerene Apex in Crystals and Liquid Crystals. *J. Am. Chem. Soc.* **2007**, *129*, 3052–3053.
39. Li, W.-S.; Yamamoto, Y.; Fukushima, T.; Saeki, A.; Seki, S.; Tagawa, S.; Masunaga, H.; Sasaki, S.; Takata, M.; Aida, T.; Amphiphilic Molecular Design as a Rational Strategy for Tailoring Bicontinuous Electron Donor and Acceptor Arrays: Photoconductive Liquid Crystalline Oligothiophene–C_{60} Dyads. *J. Am. Chem. Soc.* **2008**, *130*, 8886–8887.

40. Vergara, J.; Barberá, J.; Serrano, J. L.; Ros, M. B.; Sebastián, N.; de la Fuente, R.; López, D. O.; Fernández, G.; Sánchez, L.; Martín, N. Liquid-Crystalline Hybrid Materials Based on [60]Fullerene and Bent-Core Structures. *Angew. Chem. Int. Ed.* **2011**, *50*, 12523–12528.

41. Sawamura, M.; Iikura, H.; Nakamura, E. The First Pentahaptofullerene Metal Complexes. *J. Am. Chem. Soc.* **1996**, *118*, 12850–12851.

42. Miyazawa, K.; Kuwasaki, Y.; Obayashi, A.; Kuwabara, M. C_{60} Nanowhiskers Formed by the Liquid–Liquid Interfacial Precipitation Method. *J. Mater. Res.* **2002**, *17*, 83−88.

43. Sathish, M.; Miyazawa, K.; Hill, J. P.; Ariga, K. Solvent Engineering for Shape-Shifter Pure Fullerene (C_{60}). *J. Am. Chem. Soc.* **2009**, *131*, 6372–6373.

44. Shrestha, L. K.; Yamauchi, Y.; Hill, J. P.; Miyazawa, K.; Ariga, K. Fullerene Crystals with Bimodal Pore Architectures Consisting of Macropores and Mesopores. *J. Am. Chem. Soc.* **2013**, *135*, 586–589.

45. Rana, M.; Reddy, R. B.; Rath, B. B.; Gautam, U. K. C_{60} Mediated Molecular Shape Sorting: Separation and Purification of Geometrical Isomers. *Angew. Chem. Int. Ed.* **2014**, *53*, 13523–13527.

46 Bairi, P.; Minami, K.; Nakanishi, W.; Hill, J. P.; Ariga, K.; Shrestha, L. K. Hierarchically-Structured Fullerene C_{70} Cube for Sensing Volatile Aromatic Solvent Vapors. *ACS Nano* **2016**, *10*, 6631–6637.

47. Ruoff, R. S.; Tse, D. S.; Malhotra, R.; Lorents, D. C. Solubility of Fullerene (C_{60}) in a Variety of Solvents. *J. Phys. Chem.* **1993**, *97*, 3379–3383.

48 Ariga, K.; Minami, K.; Shrestha, L. K. Nanoarchitectonics for Carbon-material-based Sensors. *Analyst* **2016**, *141*, 2629–2638.

49. Chechetka, S. A.; Yuba, E.; Kono, K.; Yudasaka, M.; Bianco, A.; Miyako, E. Magnetically and Near-Infrared Light-Powered Supramolecular Nanotransporters for the Remote Control of Enzymatic Reactions. *Angew. Chem. Int. Ed.* **2016**, *55*, 6476–6481.

50. Miyako, E.; Chechetka, S. A.; Doi, M.; Yuba, E.; Kono, K. *In Vivo* Remote Control of Reactions in *Caenorhabditis elegans* by Using Supramolecular Nanohybrids of Carbon Nanotubes and Liposomes. *Angew. Chem. Int. Ed.* **2015**, *54*, 9903–9906.

Table of Contents Graphics